

Thermodynamic Properties of Gaseous Argon at Temperatures Between 110 and 450 K and Densities up to $6.8 \text{ mol} \cdot \text{dm}^{-3}$ Determined from the Speed of Sound

A. F. Estrada-Alexanders^{1,2} and J. P. M. Trusler^{1,3}

Received December 29, 1995

Thermodynamic properties of gaseous argon have been determined from our recent highly accurate measurements of the speed of sound by means of a numerical integration of the differential equations which link the speed of sound and the equation of state. Compression factors and both isochoric and isobaric heat capacities at temperatures between 110 and 450 K at densities up to either one-half of the critical ($T \geq 150 \text{ K}$) or 74 percent of the saturated-vapor density ($T < 150 \text{ K}$) are reported. To perform the integration, initial conditions were required along an isotherm close to the critical temperature. The method of integration is described in detail and the results are compared with pVT and calorimetric data from the literature.

KEY WORDS: argon; compression factor; equation of state; heat capacity; speed of sound.

1. INTRODUCTION

Although argon is a well-studied substance, much of the work reported in the literature was performed long ago, there are few accurate measurements of the heat capacity, and available wide-ranging equations of state are not of the highest accuracy. In view of the importance of argon as a reference

¹ Department of Chemical Engineering and Chemical Technology, Imperial College, Prince Consort Road, London SW7 2BY, United Kingdom.

² Permanent address: Departamento de Física, Universidad Autónoma Metropolitana, Apdo 55-534, CP 09340, México, D.F.

³ To whom correspondence should be addressed.

fluid, new experimental studies, using modern state-of-the-art techniques, and a thorough analysis of the thermodynamic surface are appropriate.

In a previous paper [1], we reported new speeds of sound u in gaseous argon measured in the temperature range 110 to 450 K. For $T \geq 150$ K, results were obtained at densities up to approximately $6.8 \text{ mol} \cdot \text{dm}^{-3}$ (about one half of the critical), while at lower temperatures densities up to about 80% of the saturated vapor density were studied. The estimated fractional uncertainty of these results varies from 1×10^{-5} at low densities to 7×10^{-5} at the greatest density and the temperature closest to the critical. Meanwhile, Gilgen et al. [2] have reported new measurements of the density of gaseous and liquid argon at temperatures up to 340 K and pressures to 12 MPa with an estimated fractional uncertainty of 1.5×10^{-4} . We have developed a procedure in which the speeds of sound are used to derive thermodynamic properties of the gas, including the compression factor Z and both the isochoric $C_{V,m}$ and the isobaric $C_{p,m}$ molar heat capacities, by means of a numerical integration of the differential equations which link u to the equation of state. The integration method itself has been outlined in a previous paper together with analytical and numerical calculations of the effects of errors in both the speed of sound and the initial conditions [3]. In this paper, we apply the method to argon making use of initial conditions derived from the density measurements of Gilgen et al. The results are sufficient to determine all of the observable thermodynamic properties of the gas in the entire region covered by the acoustic measurements.

2. THEORY AND NUMERICAL METHODS

The speed of sound u is related to the other thermodynamic properties through the well-known equation

$$u^2 = (\partial p / \partial \rho)_S \quad (1)$$

where p is the pressure, ρ is the mass density, and S is the entropy. Resolving the isentropic partial derivative into isothermal and isochoric terms, and introducing the compression factor $Z = p/\rho_n RT$, one obtains the equation [4]

$$u^2 = (RT/M) [\{ Z + \rho_n (\partial Z / \partial \rho_n)_T \} + (R/C_{V,m}) \{ Z + T (\partial Z / \partial T)_{\rho_n} \}^2] \quad (2)$$

where $\rho_n = \rho/M$ is the amount-of-substance density. We have consistently used in all calculations the values for the molar mass, $M = 0.0399478 \text{ kg} \cdot \text{mol}^{-1}$, and the universal gas constant, $R = 8.31451 \text{ J} \cdot \text{mol}^{-1} \cdot \text{K}^{-1}$,

that were adopted in Ref. 1. Equation (2) may be solved simultaneously with the relation

$$-(\rho_n/R)(\partial C_{v,m}/\partial \rho_n)_T = 2T(\partial Z/\partial T)_{\rho_n} + T^2(\partial^2 Z/\partial T^2)_{\rho_n} \quad (3)$$

to obtain Z and $C_{v,m}$ inside the region in which u is known. Knowledge of these quantities as functions of (T, ρ_n) is sufficient to obtain all of the other observable thermodynamic properties of the fluid; in particular, the isobaric heat capacity may be obtained from

$$(C_{p,m}/R) = (C_{v,m}/R) + \{Z + T(\partial Z/\partial T)_{\rho_n}\}^2 / \{Z + \rho_n(\partial Z/\partial \rho_n)_T\} \quad (4)$$

To perform a numerical integration of Eqs. (2) and (3), initial conditions in the form of two of the three quantities Z , $(\partial Z/\partial T)_{\rho_n}$, and $C_{v,m}$ are required along a line which crosses all of the isentropes which pass through the region of interest. In the present case, u is known in a rectangular region of T and ρ_n for $T \geq 150$ K, and, since $(\partial \rho_n/\partial T)_S > 0$ initial conditions for the integration in that region must be imposed along an isotherm near 150 K. The speed of sound is also known at temperatures below 150 K up to a roughly constant fraction of the saturated-vapor density ρ_n^σ , and since $(\partial \rho_n/\partial T)_S < (d\rho_n^\sigma/dT)$, initial conditions on an isotherm near to 150 K are appropriate for this region also.

A set of equations similar to Eq. (2) and (3) may be derived for the case in which (T, p) are the independent variables. These have been applied by Trusler and Zarari to obtain thermodynamic properties of methane at supercritical temperatures [5]. Here, we adapt the methods reported in that work for the case in which (T, ρ_n) are the independent variables and both subcritical and supercritical temperatures are encountered.

A simple predictor-corrector method was used to solve Eqs. (2) and (3) for the case of integration along a set of isochores with a positive temperature increment. Values of Z and $Z' = (\partial Z/\partial T)_{\rho_n}$ at a number of evenly spaced densities along the initial isotherm $T = T_0$ were determined as described below from the precise gas-density data of Gilgen et al. [2]. The derivative $(\partial Z/\partial \rho_n)_T$ was then calculated and combined with u and the other information on the initial isotherm to obtain $C_{v,m}$ at each density. $C_{p,m}$ was also calculated from Eq. (4). We next determined $(\partial C_{v,m}/\partial \rho_n)_T$ by numerical differentiation and thence $Z'' = (\partial^2 Z/\partial T^2)_{\rho_n}$ from Eq. (3). $Z(T_1, \rho_n)$ and $Z'(T_1, \rho_n)$ were determined at the temperature $T_1 = T_0 + \Delta T$ by means of the equations:

$$\left. \begin{aligned} Z(T_1, \rho_n) &= Z(T_1, \rho_n) + \Delta T Z'(T_0, \rho_n) + \frac{1}{2}(\Delta T)^2 Z''(T = \theta_1, \rho_n) \\ Z'(T_1, \rho_n) &= Z'(T_0, \rho_n) + \Delta T Z''(T = \theta_2, \rho_n) \end{aligned} \right\} \quad (5)$$

where $\theta_i (i = 1, 2)$ are temperatures on the interval $[T_0, T_1]$. The procedure involved first a predictor step in which θ_i was replaced by T_0 . This led to estimates of $Z(T_1, \rho_n)$ and $Z'(T_1, \rho_n)$ from which $Z''(T_1, \rho_n)$ was obtained as described above correct to $O(\Delta T^2)$. We then calculated Z'' at the mean temperature $T_m = \frac{1}{2}(T_0 + T_1)$ and, in the second (corrector) step, applied Eqs. (5) again with θ_i replaced by T_m obtaining $Z(T_1, \rho_n)$ correct to $O(\Delta T^4)$ and $Z'(T_1, \rho_n)$ correct to $O(\Delta T^3)$. These quantities then served as new initial values for the numerical integration starting from $T = T_1$. The entire procedure was repeated until the maximum temperature was reached.

The initial temperature T_0 was chosen to be 154 K and the maximum temperature was that of the experimental results, namely, 450 K. Fifty evenly spaced densities (excluding zero) up to a maximum of $6.8 \text{ mol} \cdot \text{dm}^{-3}$ were used together with a temperature increment of 0.5 K. A second short integration along the same set of isochores but with a negative temperature increment ($\Delta T = -0.1 \text{ K}$) was performed to extend the results downward in temperature to 150 K. The values of Z and Z' obtained at this temperature were used as the initial conditions for the integration in the subcritical region; there the integration proceeded downward in temperature along lines parallel to the saturation curve $\rho_n^\sigma(T)$.

All derivatives with respect to density were determined numerically by finite differences. Generally, the derivative $y'(x)$ of a function $y(x)$ known at evenly spaced ordinates $x_k = k \Delta x$ ($k = 1, 2 \dots N$) was calculated from the simple three-point formula

$$y'(x_k) = \frac{y(x_{k+1}) - y(x_{k-1}))}{2 \Delta x} + O(\Delta x^2) \quad (6)$$

neglecting the terms $O(\Delta x^2)$. This procedure was applied for all points except $k = N$. At the lowest density ($k = 1$), $y(x_{k-1})$ was set equal to the known value of y (i.e., Z or $C_{V,m}$) in the limit of zero density. At the maximum density ($k = N$), where $y(x_{k+1})$ was unavailable, $y'(x)$ was calculated from the equation

$$y'(x_N) = \frac{4y(x_N) - 7y(x_{N-1}) + 4y(x_{N-2}) - y(x_{N-3}))}{2 \Delta x} + O(\Delta x^2) \quad (7)$$

neglecting the terms $O(\Delta x^2)$. This represents a smooth extrapolation of the three-point formula rather than a full four-point finite-difference approximation to $y'(x_N)$.

Speeds of sound were required at each grid point and these were obtained by interpolation in a table of the experimental $u(T, p)$ results. It is important to note that, whenever a value was required from this table at a specified (T, ρ_n) coordinate, Z had already been evaluated there so that the corresponding (T, p) coordinate could be determined. At temperatures above 350 K, the experimental speeds of sound did not extend up to the maximum density considered here and an extrapolation was therefore required. The interpolation and extrapolation methods are described in detail below.

For the region $T \leq 150$ K, a negative temperature increment was employed and the integration proceeded not along isochores but along a set of paths evenly spaced with respect to the dimensionless variable

$$\phi = (\rho_n / \rho_n^c) / f(T) \quad (8)$$

The function $f(T)$ was chosen such that these paths were parallel to the saturated vapor density curve, $\rho_n^s(T)$, as given by McGlashan's corresponding-states correlation [6]. Thus, we set

$$f(T) = \rho_n^s(T) / \rho_n^c = 1 + 0.797(1 - T/T^c) - 1.76(1 - T/T^c)^{0.326} \quad (9)$$

where $T^c = 150.8$ K and $\rho_n^c = 13.41$ mol·dm⁻³ are the temperature and amount-of-substance density at the critical point used in the above correlation. This definition ensures that all of the isentropes which pass through the subcritical domain cross the isotherm at 150 K where initial conditions were imposed. It is not important that Eq. (9) represents accurately the true saturated vapor densities. Fifty values of ϕ were employed chosen such that each intersected at $T = 150$ K the corresponding isochore used in the supercritical region. Temperature increments of -0.01 K were used in this domain.

To facilitate the use of ϕ as an independent variable in place of ρ_n , the latter was eliminated from Eqs. (2) and (3) through the application of Eq. (8). Moreover, it was convenient to define the new molar heat capacity $C_{\phi, m} = T(\partial S_m / \partial T)_\phi$. This is related to $C_{v, m}$ and $C_{p, m}$ by the equations

$$\left. \begin{aligned} (C_{v, m} / R) &= (C_{\phi, m} / R) + T(d \ln f / dT) \{ Z + T(\partial Z / \partial T)_\phi \\ &\quad - \phi T(d \ln f / dT)(\partial Z / \partial \phi)_T \} \\ (C_{p, m} / R) &= (C_{\phi, m} / R) - T(d \ln f / dT) [Z \{ 1 + T(d \ln f / dT) \} \\ &\quad + T(\partial Z / \partial T)_\phi] \\ &\quad + [Z \{ 1 + T(d \ln f / dT) \} + T(\partial Z / \partial T)_\phi]^2 \{ Z + \phi(\partial Z / \partial \phi)_T \}^{-1} \end{aligned} \right\} \quad (10)$$

In terms of these quantities, the system of equations to be solved becomes

$$\begin{aligned}
 u^2 = & (RT/M)[C_{\phi,m}\{Z + \phi(\partial Z/\partial\phi)_T\} \\
 & + R\{Z + ZT(d \ln f/dT) + T(\partial Z/\partial T)_\phi\} \\
 & \times \{Z + T(\partial Z/\partial T)_\phi - T\phi(d \ln f/dT)(\partial Z/\partial\phi)_T\} \\
 & \times [C_{\phi,m} + RT(d \ln f/dT)\{Z + T(\partial Z/\partial T)_\phi \\
 & - T\phi(d \ln f/dT)(\partial Z/\partial\phi)_T\}]^{-1} \quad (11)
 \end{aligned}$$

and

$$\begin{aligned}
 -(\phi/R)(\partial C_{v,m}/\partial\phi)_T = & 2T(\partial Z/\partial T)_\phi + T^2(\partial^2 Z/\partial T^2)_\phi \\
 & - 2(d \ln f/d \ln T)\{\phi(\partial Z/\partial\phi)_T + T\phi(\partial^2 Z/\partial T \partial\phi)\} \\
 & + (d \ln f/d \ln T)^2 \{\phi(\partial Z/\partial\phi)_T + \phi^2(\partial^2 Z/\partial\phi^2)_T\} \quad (12)
 \end{aligned}$$

Functionally, the algorithm used to integrate these equations was the same as that described above in connection with Eqs. (2) and (3) except for the use of a negative temperature increment and the need to calculate the additional partial derivative $(\partial^2 Z/\partial T \partial\phi)$. The latter was evaluated by numerical differentiation of $(\partial Z/\partial T)_\phi$ with respect to ϕ by means of Eqs. (6) and (7) with the $\lim_{\phi \rightarrow 0}(\partial Z/\partial T)_\phi$ set to zero.

All these methods have been tested extensively through numerical simulations in which the speed of sound and the initial conditions were calculated from the equation of state of Stewart et al. [7]. Comparisons of the results with values calculated directly from the same equation of state permitted tests of the numerical accuracy of the procedures. In particular, we were able to establish appropriate values for the temperature increments and for the spacing between adjacent grid points on each isotherm. The use of 50 evenly spaced values of ρ_n or ϕ was found to be adequate for both sub- and supercritical temperatures. However, whereas $|\Delta T/K| = 0.5$ K was satisfactory for $T > T^c$, in the subcritical domain the results were independent of ΔT only when $|\Delta T/K| \leq 2 \Delta\phi \approx 0.03$. This increased sensitivity to the size of the temperature increment is attributed to the presence of the cross derivative $(\partial^2 Z/\partial T \partial\phi)$ in the differential equations. With this distribution of grid points, the numerical accuracy of the method was always better than 10^{-5} in Z and 0.001 in $C_{v,m}/R$.

The simulations support the numerical and analytical studies reported earlier [3] and confirm that the methods are stable in the sense that small errors in the initial conditions give rise to correspondingly small errors in

the solution. We also confirmed that the potentially unstable integration along isochores from 154 K down to 150 K was sufficiently short to prevent the accumulation of significant error.

3. INTERPOLATION OF THE SPEED OF SOUND

Values of the speed of sound were required at each of the 230,000 grid points used in the integration and for this purpose an interpolation algorithm was employed. Each grid point was identified by coordinates (T, ρ_n) or (T, ϕ) from which, knowing Z , the corresponding values of (T, p) were determined. $u(T, p)$ was then determined from the experimental results by two-dimensional interpolation in a table. However, rather than interpolate u itself, it was convenient to introduce an intermediate function F that varies more slowly than does u itself. This function was defined by the relation

$$F = (u/u_0)_{\text{exp}} / (u/u_0)_{\text{eos}} \quad (13)$$

where $u_0 = (5RT/3M)^{1/2}$ is the speed of sound in the limit of zero density, and subscripts denote properties obtained from either experiment or an equation of state. In the present case, $(u/u_0)_{\text{eos}}$ was obtained from the equation of Stewart et al. [7]. The ratio F was tabulated at each of the experimental state point, and once interpolated to the required grid point, the speed of sound was recovered from the relation

$$u = (5RT/3M)^{1/2} (u/u_0)_{\text{eos}} F \quad (14)$$

This method has some advantages. First, F is a smooth and slowly varying function of p and T inside the whole experimental region and never deviates from unity by more than 2.6×10^{-2} . Second, Eqs. (13) and (14) ensure that $u \rightarrow (5RT/3M)^{1/2}$ exactly as $p \rightarrow 0$ while (u/u_0) agrees exactly with $(u/u_0)_{\text{exp}}$ at each of the experimental state points.

Even though F is a fairly slowly varying function of (T, p) , it proved to be advantageous to perform a change of variables from (T, p) to (τ, ω) , where $\tau = 1/T$ and $\omega = \rho_n^{\text{eos}}(T, p) / \rho_n^c$ is the reduced density calculated from the equation of state at the state point specified by (T, p) . Two-dimensional interpolation in a table of $F(\tau, \omega)$ was therefore the procedure used in practice. To improve the computational efficiency, a partial interpolation in ω was first performed on each isotherm by means of the six-point Lagrange formula. This lead to values of F on each of the isotherms with even spacing $\Delta\omega = 0.004$, in place of the unevenly spaced experimental points with $\Delta\omega \approx 0.05$, and a table of these values was used routinely. Further interpolation with respect to ω required only a two-point formula to hold

the truncation error below $10^{-6}F$. Interpolation with respect to τ was performed by means of the six-point Lagrange formula.

We are entirely satisfied with the interpolations over ω , which, given the spacing of the experimental speeds of sound on each isotherm, appears to involve negligible additional uncertainty. Comparison with the results of a five-point interpolation reveal noticeable ripple only near to the greatest density on the isotherm at 150 K; even here the ripple amounts to only about 10×10^{-6} in the function F . However, similar comparisons for the interpolation over τ reveal ripples of that order over a substantial region of the surface increasing to about $20 \cdot 10^{-6}$ at the greatest density near to the critical temperature. Although this is still too little to affect the derived compression factors by more than 2×10^{-5} , there are some noticeable consequences for the heat capacities which we discuss in more detail below.

Except at 400 and 450 K, the greatest experimental density on each isotherm corresponds to $\omega \geq 0.5$. However, at 400 K the greatest density corresponds to $\omega = 0.41$, while, at 450 K, the results reach just $\omega = 0.37$. For these two isotherms, the function F was extrapolated to $\omega = 0.5$ by means of a rational approximation $F(\omega) \approx R(\omega) = P_{2n}(\omega)/Q_{2n}(\omega)$ in which $P_{2n}(\omega)$ and $Q_{2n}(\omega)$ are polynomials of degree n in ω with constant terms set equal to unity. The coefficients of these polynomials were chosen such that $R(\omega)$ was identical with $F(\omega)$ at the last $2n$ experimental points on the isotherm ranked in order of increasing ω . At 400 K, $n = 2$ appeared to be adequate, while at 450 K, we preferred $n = 3$. The switch from six-point interpolation over ω to the rational approximation was made at the greatest experimental value of ω , ω_{\max} , to ensure continuity of F . The poles of the rational functions were analysed to ensure that they were outside of the region $\omega_{\max} \leq \omega \leq 0.5$. The main purpose of the extrapolations was to complete the table of $F(\tau, \omega)$ in a way that would permit accurate interpolation within the experimental region. Nevertheless, we believe that the rational approximation is sufficiently accurate to warrant giving results for derived properties in the extrapolated region too. This region corresponds roughly to the domain $p \geq 20$ MPa.

4. INITIAL CONDITIONS

Initial values of Z and Z' , hereafter denoted Z_0 and Z'_0 , were required on the isotherm $T = T_0$. To the best of our knowledge, the recent density measurements of Gilgen et al. provide the most accurate experimental evidence upon which to base the initial conditions and we have chosen three of their isotherms for this purpose. Two of these, the isotherms at 153 and 155 K, are located symmetrically above and below the initial temperature of 154 K. Values of Z on each of these two isotherms at densities

up to $7 \text{ mol} \cdot \text{dm}^{-3}$ were fitted to polynomials of the fourth degree in ρ_n restricted to be exactly unity in the limit of zero density. The precision of the measurements in this regime is clearly much higher than the estimated overall uncertainty of $1.5 \text{ to } 2 \times 10^{-4} Z$ and the greatest deviation from our fits was just $1 \times 10^{-5} \cdot Z_0$ and Z'_0 were then estimated by means of the relations

$$Z_0 = 2^{-1}(Z_2 + Z_1) - (2!)^{-1} (\Delta T)^2 Z''_0 + \dots \quad (15)$$

and

$$Z'_0 = (2 \Delta T)^{-1} (Z_2 - Z_1) - (3!)^{-1} (\Delta T)^2 Z'''_0 + \dots \quad (16)$$

where $\Delta T = 1 \text{ K}$, and Z_1 and Z_2 denote the polynomial approximations to Z at $T_1 = 153 \text{ K}$ and $T_2 = 155 \text{ K}$. Equation (15) truncated after the leading term is already nearly accurate enough for our purpose, but it turned out to be quite straightforward to include the second temperature derivative Z''_0 by means of the following procedure. First, only the terms in Z_1 and Z_2 were retained leading to approximate values of Z_0 and Z'_0 which, when substituted in Eqs. (2) and (3), gave an approximation to Z''_0 . Then Eq. (15) was applied again to obtain an improved estimate of Z_0 . Iterations of this procedure converged rapidly to give consistent values of Z and the first two temperature derivatives at $T = T_0$. The greatest contribution of the second derivative term in Eq. (15) is just 6.3×10^{-5} and we are satisfied that the procedure provides values of Z_0 with an accuracy equal to that of the original experimental results at T_1 and T_2 .

The situation with regard to Z'_0 is less satisfactory. To prevent this term from dominating the overall uncertainty of the results, it is desirable that $T_0 Z'_0$ be burdened by an error not greater than that of Z_0 itself, say about $\pm 2 \times 10^{-4}$ in absolute terms. The accuracy with which Z'_0 may be obtained is affected both by errors in $(Z_2 - Z_1)$ and by the truncation of Eq. (16). We expect that systematic errors present in the original experimental results will cancel to a large extent in the difference $(Z_2 - Z_1)$ so that this term will be associated with an uncertainty of the same order as the precision of Z itself. However, this still implies an uncertainty in $T_0 Z'_0$ of order 10^{-3} , which is about a factor of five too large. Compared with this uncertainty, the truncation error introduced by neglecting the third and higher temperature derivatives in Eq. (16) is insignificant. However, we note in passing that these derivatives may be determined in principle by requiring consistency between the values used in the estimation of the initial conditions and those subsequently obtained from the integration of u .

Several strategies were considered by which an improved estimate of Z'_0 could be obtained. One was the inclusion of more isotherms near to T_0 , but although these could be used to eliminate higher derivatives of Z from the problem, the reduction in the overall uncertainty would be marginal. Instead, we note that the error ε associated with the approximation

$$Z'_0 \approx (2 \Delta T)^{-1} (Z_2 - Z_1) \quad (17)$$

must itself be a polynomial in ρ_n . The form of the polynomials Z_1 and Z_2 automatically ensures that the constant term in ε is exactly zero so that the leading term is $b\rho_n$. It is known that small error terms in Z'_0 proportional to positive powers of ρ_n give rise to errors in the solution which at first grow before reaching a maximum at some temperature above T_0 and then decaying [3]. In the present case, the consequences of the term $b\rho_n$ reach a maximum at about 200 K, while higher terms are much less important and have propagated errors which peak at temperatures closer to the initial isotherm. Furthermore, $(Z_2 - Z_1)$ is remarkably close to a linear function of ρ_n in the present range of densities. These observations suggest that a substantial improvement to Eq. (17) may be achieved by the addition to the right-hand side of a term $b\rho_n$ with the parameter b adjusted so that the compression factors obtained upon integration of u agree with experiment on an isotherm near to 200 K. An almost-equivalent procedure is to multiply $(Z_2 - Z_1)$ by a constant term $(1 + \delta)$ with δ adjusted using the same criterion. This was the strategy used in practise and optimization by comparison with the isotherm of Gilgen et al. at $T_3 = 220$ K gave $\delta = 6.8 \times 10^{-4}$. The effect of this adjustment was to increase Z'_0 by about $5 \times 10^{-6} \text{ K}^{-1}$ at the greatest density and is equivalent to a change of only 10^{-5} in either Z_1 or Z_2 at the same density; consequently, we can say that the adjusted derivative is equally consistent with the experimental density data at T_1 and T_2 .

In summary, the initial conditions Z_0 and Z'_0 were established mainly on the basis of independent measurements of gas density on two isotherms near T_0 but with an empirical adjustment based on results at a third temperature. We note that, in contrast to the present case, many polyatomic gases have heat capacities which are sufficiently large that errors of order 10^{-3} in $T_0 Z'_0$ could be tolerated; two independent isotherms may then be sufficient.

5. DETERMINATION OF THE HEAT CAPACITIES

One unexpected problem came to light during the integration. After the preliminary analysis, it was found that, with increasing temperature along an isochore, small ripples appeared in the derived values of $C_{\nu,m}$.

These ripples became quite obvious by the highest temperatures where $C_{V,m}$ increases by only $0.08 R$ between zero density and $\rho_n = 6.8 \text{ mol} \cdot \text{dm}^{-3}$. At that temperature, the amplitude of the ripples was about $0.002 R$, which, although small, was easily detected graphically.

Evidence obtained from simulations indicates that the origin of these ripples is small oscillatory errors in the interpolated speeds of sound. When in a simulation u was perturbed by a fractional error in the form of a sinusoidal function whose argument was a linear combination of the interpolating variables, τ and ω , similar oscillations appeared in $C_{V,m}$. It appears that an amplitude of about $30 \times 10^{-6} u$ yields ripples in $C_{V,m}$ similar to those observed in practice with little effect ($<0.01\%$) on the derived values of Z .

To overcome this difficulty, the values of $C_{V,m}$ determined on each isotherm during the integration were smoothed by means of a fourth-degree polynomial in ρ_n before the next temperature step was taken. This smoothing acted as an effective filter, preventing the growth of noticeable ripples in $C_{V,m}$ but, at the same time, not altering the derived values of Z significantly. In fact, the greatest change in Z , just 8×10^{-5} , was found at the highest temperature and density. The isobaric heat capacity $C_{p,m}$ was obtained from the smoothed values of $C_{V,m}$ by means of Eq. (4); this ensured that all the heat capacities (isobaric and isochoric) were smooth functions in the whole supercritical region. The results obtained with smoothing were found to agree with the previous results to within the amplitude of the ripples in the latter. No evidence of ripples in $C_{V,m}$ were found during the integration in the subcritical region, and consequently, the filter was not used there.

6. RESULTS

The derived thermodynamic properties of argon (Z , $C_{V,m}$, and $C_{p,m}$) are given in Table I at selected temperatures and densities. Sufficient information is given to obtain values at intermediate state points without loss of accuracy by quadratic interpolation even in the case of a bidimensional interpolation in T and ρ_n near the critical temperature. In Figs. 1–3, we show the compression factors obtained from the measurements of Gilgen et al. [2] as deviations from the surface derived from our speeds of sound. The agreement is seen to be excellent at both subcritical and supercritical temperatures, with a mean deviation of 0.003% and a root-mean-square deviation of 0.01% . Based on these comparisons we estimate that the uncertainty of the compression factors reported here is no worse than $\pm 0.025\%$. We also estimate that the uncertainty of the derived heat capacities is not more than $\pm 0.1\%$ except near T^c , where the uncertainty

Table I. Thermodynamic Properties of Argon Derived from the Speed of Sound^a

ρ_n (mol · dm ⁻³)	Z	$C_{v,m}/R$	$C_{p,m}/R$	ρ_n (mol · dm ⁻³)	Z	$C_{v,m}/R$	$C_{p,m}/R$
T = 110.0 K							
0.025	0.996159	1.5060	2.5202	0.350	0.946419	1.5906	2.8178
0.050	0.992320	1.5120	2.5407	0.375	0.942603	1.5978	2.8439
0.075	0.988482	1.5181	2.5617	0.400	0.938789	1.6047	2.8698
0.100	0.984649	1.5242	2.5827	0.425	0.934980	1.6116	2.8958
0.125	0.980818	1.5303	2.6042	0.450	0.931174	1.6185	2.9223
0.150	0.976989	1.5367	2.6262	0.475	0.927371	1.6258	2.9499
0.175	0.973159	1.5433	2.6490	0.500	0.923570	1.6335	2.9786
0.200	0.969329	1.5500	2.6722	0.525	0.919768	1.6413	3.0080
0.225	0.965504	1.5566	2.6955	0.550	0.915966	1.6492	3.0380
0.250	0.961683	1.5631	2.7186	0.575	0.912165	1.6571	3.0682
0.275	0.957866	1.5696	2.7422	0.600	0.908365	1.6650	3.0990
0.300	0.954051	1.5763	2.7665	0.625	0.904566	1.6732	3.1307
0.325	0.950236	1.5834	2.7918				
T = 115.0 K							
0.034	0.995187	1.5068	2.5247	0.476	0.933050	1.6092	2.9026
0.068	0.990378	1.5139	2.5501	0.510	0.928302	1.6176	2.9358
0.102	0.985575	1.5212	2.5762	0.544	0.923560	1.6257	2.9694
0.136	0.980778	1.5283	2.6024	0.578	0.918822	1.6342	3.0041
0.170	0.975984	1.5355	2.6292	0.612	0.914088	1.6433	3.0404
0.204	0.971195	1.5430	2.6569	0.646	0.909356	1.6528	3.0781
0.238	0.966411	1.5510	2.6855	0.680	0.904627	1.6625	3.1166
0.272	0.961632	1.5590	2.7145	0.714	0.899901	1.6720	3.1556
0.306	0.956859	1.5670	2.7439	0.748	0.895179	1.6814	3.1951
0.340	0.952091	1.5749	2.7739	0.782	0.890461	1.6911	3.2359
0.374	0.947325	1.5830	2.8047	0.816	0.885747	1.7014	3.2783
0.408	0.942563	1.5916	2.8367	0.850	0.881035	1.7121	3.3223
0.442	0.937804	1.6004	2.8695				
T = 120.0 K							
0.044	0.994242	1.5082	2.5298	0.616	0.920190	1.6256	2.9873
0.088	0.988493	1.5165	2.5602	0.660	0.914554	1.6355	3.0290
0.132	0.982754	1.5250	2.5913	0.704	0.908926	1.6457	3.0722
0.176	0.977023	1.5336	2.6232	0.748	0.903304	1.6562	3.1166
0.220	0.971301	1.5422	2.6558	0.792	0.897690	1.6668	3.1623
0.264	0.965588	1.5510	2.6891	0.836	0.892083	1.6775	3.2092
0.308	0.959884	1.5598	2.7231	0.880	0.886483	1.6883	3.2573
0.352	0.954189	1.5688	2.7580	0.924	0.880891	1.6993	3.3067
0.396	0.948502	1.5779	2.7939	0.968	0.875307	1.7105	3.3577
0.440	0.942823	1.5872	2.8307	1.012	0.869730	1.7220	3.4105
0.484	0.937151	1.5966	2.8685	1.056	0.864159	1.7338	3.4650
0.528	0.931488	1.6062	2.9072	1.100	0.858595	1.7457	3.5212
0.572	0.925835	1.6158	2.9467				

^a To permit accurate interpolation, results are given here to more significant figures than are justified by the accuracy claimed.

Table I. (Continued)

ρ_n (mol · dm ⁻³)	Z	$C_{v,m}/R$	$C_{p,m}/R$	ρ_n (mol · dm ⁻³)	Z	$C_{v,m}/R$	$C_{p,m}/R$
<i>T</i> = 125.0 K							
0.057	0.993085	1.5096	2.5356	0.798	0.904588	1.6460	3.0981
0.114	0.986186	1.5192	2.5721	0.855	0.897885	1.6578	3.1513
0.171	0.979303	1.5290	2.6095	0.912	0.891196	1.6699	3.2064
0.228	0.972435	1.5390	2.6480	0.969	0.884520	1.6823	3.2633
0.285	0.965582	1.5491	2.6876	1.026	0.877858	1.6947	3.3220
0.342	0.958744	1.5593	2.7281	1.083	0.871211	1.7073	3.3825
0.399	0.951922	1.5695	2.7698	1.140	0.864577	1.7201	3.4452
0.456	0.945115	1.5799	2.8126	1.197	0.857957	1.7332	3.5103
0.513	0.938322	1.5905	2.8568	1.254	0.851351	1.7467	3.5779
0.570	0.931545	1.6014	2.9024	1.311	0.844757	1.7605	3.6481
0.627	0.924783	1.6123	2.9491	1.368	0.838177	1.7746	3.7209
0.684	0.918036	1.6234	2.9973	1.425	0.831610	1.7889	3.7965
0.741	0.911305	1.6345	3.0468				
<i>T</i> = 130.0 K							
0.073	0.991769	1.5109	2.5421	1.022	0.887082	1.6687	3.2327
0.146	0.983564	1.5220	2.5855	1.095	0.879204	1.6825	3.3002
0.219	0.975385	1.5332	2.6302	1.168	0.871350	1.6965	3.3703
0.292	0.967231	1.5445	2.6764	1.241	0.863521	1.7108	3.4432
0.365	0.959103	1.5561	2.7240	1.314	0.855716	1.7253	3.5191
0.438	0.950999	1.5678	2.7732	1.387	0.847935	1.7403	3.5982
0.511	0.942921	1.5797	2.8240	1.460	0.840178	1.7555	3.6807
0.584	0.934869	1.5918	2.8765	1.533	0.832445	1.7711	3.7667
0.657	0.926841	1.6041	2.9307	1.606	0.824736	1.7871	3.8566
0.730	0.918840	1.6165	2.9868	1.679	0.817051	1.8035	3.9506
0.803	0.910863	1.6292	3.0449	1.752	0.809391	1.8203	4.0490
0.876	0.902912	1.6421	3.1052	1.825	0.801753	1.8376	4.1524
0.949	0.894985	1.6553	3.1677				
<i>T</i> = 135.0 K							
0.094	0.990128	1.5127	2.5505	1.316	0.865605	1.6974	3.4150
0.188	0.980298	1.5255	2.6028	1.410	0.856318	1.7137	3.5033
0.282	0.970510	1.5385	2.6569	1.504	0.847074	1.7303	3.5956
0.376	0.960763	1.5517	2.7131	1.598	0.837871	1.7472	3.6924
0.470	0.951059	1.5652	2.7713	1.692	0.828711	1.7646	3.7941
0.564	0.941396	1.5788	2.8319	1.786	0.819592	1.7825	3.9009
0.658	0.931776	1.5927	2.8948	1.880	0.810515	1.8008	4.0133
0.752	0.922197	1.6069	2.9601	1.974	0.801479	1.8196	4.1318
0.846	0.912661	1.6212	3.0281	2.068	0.792485	1.8390	4.2569
0.940	0.903166	1.6358	3.0989	2.162	0.783533	1.8590	4.3890
1.034	0.893713	1.6506	3.1728	2.256	0.774621	1.8796	4.5287
1.128	0.884302	1.6659	3.2500	2.350	0.765752	1.9008	4.6765
1.222	0.874933	1.6815	3.3307				

Table I. (Continued)

ρ_n (mol · dm ⁻³)	Z	$C_{V,m}/R$	$C_{p,m}/R$	ρ_n (mol · dm ⁻³)	Z	$C_{V,m}/R$	$C_{p,m}/R$
<i>T</i> = 140.0 K							
0.123	0.987945	1.5151	2.5618	1.722	0.837675	1.7367	3.6855
0.246	0.975960	1.5303	2.6263	1.845	0.826618	1.7565	3.8071
0.369	0.964046	1.5458	2.6935	1.968	0.815633	1.7769	3.9358
0.492	0.952202	1.5616	2.7637	2.091	0.804722	1.7977	4.0724
0.615	0.940428	1.5776	2.8372	2.214	0.793884	1.8192	4.2174
0.738	0.928726	1.5939	2.9140	2.337	0.783119	1.8413	4.3715
0.861	0.917094	1.6105	2.9944	2.460	0.772428	1.8641	4.5357
0.984	0.905534	1.6273	3.0787	2.583	0.761811	1.8876	4.7107
1.107	0.894045	1.6445	3.1672	2.706	0.751268	1.9118	4.8977
1.230	0.882627	1.6621	3.2603	2.829	0.740800	1.9368	5.0977
1.353	0.871281	1.6801	3.3583	2.952	0.730407	1.9626	5.3123
1.476	0.870007	1.6985	3.4615	3.075	0.720089	1.9893	5.5427
1.599	0.848805	1.7173	3.5704				
<i>T</i> = 145.0 K							
0.167	0.984704	1.5186	2.5789	2.338	0.797537	1.7977	4.1549
0.334	0.969533	1.5374	2.6620	2.505	0.784065	1.8234	4.3414
0.501	0.954489	1.5566	2.7496	2.672	0.770728	1.8498	4.5423
0.668	0.939571	1.5762	2.8422	2.839	0.757529	1.8771	4.7588
0.835	0.924781	1.5962	2.9401	3.006	0.744467	1.9052	4.9926
1.002	0.910120	1.6165	3.0437	3.173	0.731544	1.9342	5.2457
1.169	0.895587	1.6373	3.1537	3.340	0.718760	1.9642	5.5203
1.336	0.881184	1.6584	3.2704	3.507	0.706116	1.9952	5.8191
1.503	0.866912	1.6801	3.3947	3.674	0.693613	2.0275	6.1450
1.670	0.852771	1.7024	3.5271	3.841	0.681251	2.0609	6.5012
1.837	0.838763	1.7253	3.6684	4.008	0.669032	2.0957	6.8919
2.004	0.824887	1.7487	3.8195	4.175	0.656957	2.1319	7.3215
2.171	0.811145	1.7729	3.9813				
<i>T</i> = 147.5 K							
0.202	0.982109	1.5216	2.5929	2.828	0.766489	1.8496	4.6011
0.404	0.964398	1.5435	2.6915	3.030	0.751258	1.8803	4.8568
0.606	0.946869	1.5658	2.7964	3.232	0.736228	1.9120	5.1358
0.808	0.929524	1.5885	2.9081	3.434	0.721401	1.9448	5.4411
1.010	0.912364	1.6116	3.0275	3.636	0.706776	1.9787	5.7758
1.212	0.895391	1.6353	3.1551	3.838	0.692357	2.0137	6.1439
1.414	0.878605	1.6596	3.2919	4.040	0.678144	2.0501	6.5499
1.616	0.862009	1.6845	3.4388	4.242	0.664139	2.0878	6.9991
1.818	0.845604	1.7100	3.5969	4.444	0.650343	2.1271	7.4977
2.020	0.829391	1.7363	3.7672	4.646	0.636757	2.1679	8.0529
2.222	0.813371	1.7633	3.9513	4.848	0.623383	2.2104	8.6736
2.424	0.797547	1.7912	4.1504	5.050	0.610221	2.2547	9.3704
2.626	0.781919	1.8199	4.3664				

Table I. (Continued)

ρ_n (mol · dm ⁻³)	Z	$C_{v,m}/R$	$C_{p,m}/R$	ρ_n (mol · dm ⁻³)	Z	$C_{v,m}/R$	$C_{p,m}/R$
<i>T</i> = 150.0 K							
0.272	0.976716	1.5276	2.6220	3.808	0.704737	1.9702	5.8014
0.544	0.953754	1.5558	2.7541	4.080	0.686300	2.0134	6.2769
0.816	0.931119	1.5848	2.8973	4.352	0.668234	2.0583	6.8134
1.088	0.908815	1.6145	3.0532	4.624	0.650541	2.1052	7.4210
1.360	0.886845	1.6451	3.2233	4.896	0.633224	2.1540	8.1122
1.632	0.865212	1.6766	3.4093	5.168	0.616286	2.2050	8.9016
1.904	0.843922	1.7091	3.6133	5.440	0.599731	2.2582	9.8075
2.176	0.822976	1.7426	3.8377	5.712	0.583559	2.3138	10.8522
2.448	0.802379	1.7772	4.0852	5.984	0.567775	2.3719	12.0633
2.720	0.782134	1.8131	4.3590	6.256	0.552380	2.4326	13.4752
2.992	0.762244	1.8502	4.6628	6.528	0.537377	2.4962	15.1312
3.264	0.742712	1.8887	5.0009	6.800	0.522767	2.5626	17.0859
3.536	0.723543	1.9286	5.3785				
<i>T</i> = 150.7 K							
0.272	0.976924	1.5273	2.6210	3.808	0.707516	1.9604	5.7298
0.544	0.954169	1.5552	2.7518	4.080	0.689265	2.0022	6.1879
0.816	0.931739	1.5838	2.8935	4.352	0.671383	2.0456	6.7028
1.088	0.909638	1.6130	3.0474	4.624	0.653873	2.0906	7.2834
1.360	0.887870	1.6431	3.2151	4.896	0.636736	2.1375	7.9404
1.632	0.866438	1.6740	3.3983	5.168	0.619976	2.1861	8.6867
1.904	0.845347	1.7058	3.5988	5.440	0.603595	2.2367	9.5377
2.176	0.824599	1.7386	3.8191	5.712	0.587596	2.2893	10.5121
2.448	0.804199	1.7725	4.0616	5.984	0.571908	2.3439	11.6326
2.720	0.784149	1.8075	4.3293	6.256	0.556750	2.4008	12.9268
2.992	0.764452	1.8438	4.6256	6.528	0.541908	2.4599	14.4288
3.264	0.745112	1.8813	4.9546	6.800	0.527457	2.5214	16.1804
3.536	0.726133	1.9201	5.3208				
<i>T</i> = 152.5 K							
0.272	0.977448	1.5266	2.6184	3.808	0.714489	1.9369	5.5594
0.544	0.955212	1.5536	2.7459	4.080	0.696704	1.9755	5.9777
0.816	0.933298	1.5811	2.8837	4.352	0.679282	2.0152	6.4435
1.088	0.911709	1.6092	3.0328	4.624	0.662226	2.0562	6.9634
1.360	0.890449	1.6380	3.1948	4.896	0.645537	2.0985	7.5449
1.632	0.869521	1.6675	3.3710	5.168	0.629218	2.1420	8.1972
1.904	0.848930	1.6978	3.5633	5.440	0.613271	2.1867	8.9304
2.176	0.828679	1.7289	3.7736	5.712	0.597697	2.2328	9.7568
2.448	0.808771	1.7610	4.0040	5.984	0.582499	2.2801	10.6904
2.720	0.789210	1.7941	4.2570	6.256	0.567677	2.3287	11.7476
2.992	0.769998	1.8281	4.5356	6.528	0.553234	2.3786	12.9472
3.264	0.751138	1.8633	4.8429	6.800	0.539170	2.4297	14.3113
3.536	0.732634	1.8995	5.1828				

Table I. (Continued)

ρ_n (mol · dm ⁻³)	Z	$C_{V,m}/R$	$C_{p,m}/R$	ρ_n (mol · dm ⁻³)	Z	$C_{V,m}/R$	$C_{p,m}/R$
$T = 155.0$ K							
0.272	0.978149	1.5255	2.6148	3.808	0.723785	1.9078	5.3507
0.544	0.956609	1.5513	2.7380	4.080	0.706616	1.9426	5.7230
0.816	0.935384	1.5775	2.8706	4.352	0.689803	1.9781	6.1330
1.088	0.914479	1.6041	3.0137	4.624	0.673346	2.0145	6.5851
1.360	0.893898	1.6313	3.1683	4.896	0.657248	2.0516	7.0843
1.632	0.873643	1.6591	3.3357	5.168	0.641510	2.0895	7.6360
1.904	0.853720	1.6875	3.5175	5.440	0.626133	2.1280	8.2466
2.176	0.834131	1.7166	3.7152	5.712	0.611119	2.1672	8.9227
2.448	0.814879	1.7465	3.9306	5.984	0.596467	2.2069	9.6722
2.720	0.795968	1.7771	4.1657	6.256	0.582179	2.2472	10.5032
2.992	0.777401	1.8085	4.4225	6.528	0.568256	2.2879	11.4247
3.264	0.759179	1.8408	4.7038	6.800	0.554697	2.3289	12.4464
3.536	0.741306	1.8739	5.0121				
$T = 157.5$ K							
0.272	0.978822	1.5245	2.6114	3.808	0.732662	1.8821	5.1688
0.544	0.957948	1.5491	2.7306	4.080	0.716079	1.9137	5.5034
0.816	0.937384	1.5741	2.8584	4.352	0.699842	1.9458	5.8684
1.088	0.917134	1.5994	2.9957	4.624	0.683954	1.9784	6.2668
1.360	0.897202	1.6252	3.1436	4.896	0.668414	2.0115	6.7020
1.632	0.877592	1.6514	3.3032	5.168	0.653226	2.0449	7.1774
1.904	0.858306	1.6781	3.4755	5.440	0.638388	2.0787	7.6968
2.176	0.839349	1.7054	3.6620	5.712	0.623901	2.1128	8.2643
2.448	0.820724	1.7333	3.8641	5.984	0.609766	2.1470	8.8840
2.720	0.802433	1.7618	4.0833	6.256	0.595982	2.1814	9.5604
2.992	0.784479	1.7910	4.3214	6.528	0.582549	2.2157	10.2979
3.264	0.766864	1.8207	4.5802	6.800	0.569467	2.2498	11.1008
3.536	0.749591	1.8511	4.8620				
$T = 160.0$ K							
0.272	0.979467	1.5235	2.6081	3.808	0.741154	1.8592	5.0088
0.544	0.959233	1.5471	2.7235	4.080	0.725127	1.8881	5.3119
0.816	0.939303	1.5709	2.8469	4.352	0.709439	1.9173	5.6399
1.088	0.919681	1.5951	2.9790	4.624	0.694091	1.9468	5.9949
1.360	0.900371	1.6195	3.1207	4.896	0.679083	1.9766	6.3791
1.632	0.881377	1.6444	3.2730	5.168	0.664416	2.0066	6.7948
1.904	0.862702	1.6696	3.4368	5.440	0.650090	2.0367	7.2442
2.176	0.844350	1.6953	3.6132	5.712	0.636105	2.0668	7.7299
2.448	0.826323	1.7215	3.8034	5.984	0.622461	2.0969	8.2541
2.720	0.808624	1.7481	4.0087	6.256	0.609156	2.1268	8.8191
2.992	0.791255	1.7752	4.2303	6.528	0.596190	2.1565	9.4272
3.264	0.774220	1.8027	4.4698	6.800	0.583562	2.1857	10.0803
3.536	0.757518	1.8308	4.7287				

Table I. (Continued)

ρ_n (mol · dm ⁻³)	Z	$C_{V,m}/R$	$C_{p,m}/R$	ρ_n (mol · dm ⁻³)	Z	$C_{V,m}/R$	$C_{p,m}/R$
<i>T</i> = 175.0 K							
0.680	0.957629	1.5469	2.7389	4.080	0.772229	1.7802	4.5328
1.360	0.916963	1.5935	3.0108	4.760	0.740648	1.8263	5.0451
2.040	0.878054	1.6401	3.3211	5.440	0.710914	1.8712	5.6159
2.720	0.840944	1.6869	3.6748	6.120	0.683011	1.9144	6.2443
3.400	0.805663	1.7336	4.0772	6.800	0.656908	1.9550	6.9264
<i>T</i> = 190.0 K							
0.680	0.964383	1.5383	2.7053	4.080	0.809956	1.7167	4.0896
1.360	0.930295	1.5757	2.9327	4.760	0.783978	1.7494	4.4415
2.040	0.897778	1.6123	3.1839	5.440	0.759653	1.7806	4.8154
2.720	0.866868	1.6481	3.4601	6.120	0.736970	1.8103	5.2075
3.400	0.837589	1.6829	3.7621	6.800	0.715910	1.8380	5.6132
<i>T</i> = 205.0 K							
0.680	0.969927	1.5320	2.6795	4.080	0.840989	1.6755	3.8034
1.360	0.941243	1.5630	2.8744	4.760	0.819648	1.7005	4.0674
2.040	0.913982	1.5929	3.0848	5.440	0.799820	1.7241	4.3394
2.720	0.888171	1.6217	3.3104	6.120	0.781506	1.7464	4.6161
3.400	0.863834	1.6492	3.5504	6.800	0.764704	1.7672	4.8941
<i>T</i> = 220.0 K							
0.680	0.974557	1.5274	2.6593	4.080	0.867012	1.6472	3.6035
1.360	0.950393	1.5537	2.8295	4.760	0.849594	1.6674	3.8130
2.040	0.927532	1.5789	3.0100	5.440	0.833581	1.6863	4.0245
2.720	0.906001	1.6029	3.2001	6.120	0.818989	1.7040	4.2352
3.400	0.885820	1.6257	3.3985	6.800	0.805829	1.7205	4.4424
<i>T</i> = 235.0 K							
0.680	0.978479	1.5238	2.6429	4.080	0.889164	1.6267	3.4559
1.360	0.958148	1.5466	2.7937	4.760	0.875114	1.6438	3.6289
2.040	0.939029	1.5683	2.9515	5.440	0.862388	1.6597	3.8010
2.720	0.921144	1.5890	3.1155	6.120	0.851010	1.6745	3.9699
3.400	0.904515	1.6084	3.2841	6.800	0.841001	1.6882	4.1336
<i>T</i> = 250.0 K							
0.680	0.981840	1.5209	2.6294	4.080	0.908249	1.6113	3.3424
1.360	0.964801	1.5410	2.7645	4.760	0.897128	1.6262	3.4894
2.040	0.948901	1.5601	2.9045	5.440	0.887265	1.6401	3.6340
2.720	0.934161	1.5782	3.0484	6.120	0.878693	1.6530	3.7745
3.400	0.920602	1.5953	3.1948	6.800	0.871439	1.6649	3.9093

Table I. (Continued)

ρ_n (mol · dm ⁻³)	Z	$C_{V,m}/R$	$C_{p,m}/R$	ρ_n (mol · dm ⁻³)	Z	$C_{V,m}/R$	$C_{p,m}/R$
<i>T</i> = 265.0 K							
0.680	0.984751	1.5186	2.6181	4.080	0.924857	1.5994	3.2523
1.360	0.970567	1.5365	2.7403	4.760	0.916305	1.6128	3.3799
2.040	0.957465	1.5536	2.8660	5.440	0.908961	1.6253	3.5045
2.720	0.945463	1.5698	2.9940	6.120	0.902860	1.6368	3.6246
3.400	0.934586	1.5851	3.1232	6.800	0.898038	1.6476	3.7391
<i>T</i> = 280.0 K							
0.680	0.987294	1.5167	2.6085	4.080	0.939432	1.5900	3.1792
1.360	0.975609	1.5329	2.7200	4.760	0.933152	1.6023	3.2918
2.040	0.964959	1.5484	2.8338	5.440	0.928040	1.6137	3.4011
2.720	0.955364	1.5631	2.9490	6.120	0.924133	1.6243	3.5059
3.400	0.946846	1.5770	3.0645	6.800	0.921471	1.6342	3.6053
<i>T</i> = 295.0 K							
0.680	0.989534	1.5152	2.6002	4.080	0.952318	1.5824	3.1185
1.360	0.980051	1.5299	2.7027	4.760	0.948061	1.5938	3.2192
2.040	0.971567	1.5441	2.8066	5.440	0.944938	1.6044	3.3165
2.720	0.964101	1.5576	2.9112	6.120	0.942991	1.6143	3.4095
3.400	0.957675	1.5703	3.0155	6.800	0.942260	1.6236	3.4974
<i>T</i> = 310.0 K							
0.680	0.991520	1.5140	2.5931	4.080	0.963784	1.5761	3.0673
1.360	0.983993	1.5275	2.6878	4.760	0.961337	1.5868	3.1584
2.040	0.977434	1.5405	2.7833	5.440	0.959999	1.5968	3.2461
2.720	0.971862	1.5530	2.8789	6.120	0.959810	1.6063	3.3296
3.400	0.967303	1.5649	2.9739	6.800	0.960815	1.6151	3.4084
<i>T</i> = 325.0 K							
0.680	0.993292	1.5129	2.5869	4.080	0.974044	1.5709	3.0236
1.360	0.987511	1.5254	2.6748	4.760	0.973225	1.5810	3.1066
2.040	0.982673	1.5375	2.7631	5.440	0.973495	1.5906	3.1864
2.720	0.978799	1.5491	2.8511	6.120	0.974893	1.5996	3.2623
3.400	0.975912	1.5603	2.9382	6.800	0.977466	1.6082	3.3338
<i>T</i> = 340.0 K							
0.680	0.994882	1.5120	2.5814	4.080	0.983271	1.5665	2.9859
1.360	0.990668	1.5237	2.6634	4.760	0.983924	1.5761	3.0621
2.040	0.987377	1.5350	2.7454	5.440	0.985648	1.5853	3.1352
2.720	0.985030	1.5459	2.8270	6.120	0.988484	1.5941	3.2048
3.400	0.983651	1.5564	2.9073	6.800	0.992479	1.6025	3.2703

Table I. (Continued)

ρ_n (mol · dm ⁻³)	Z	$C_{V,m}/R$	$C_{p,m}/R$	ρ_n (mol · dm ⁻³)	Z	$C_{V,m}/R$	$C_{p,m}/R$
<i>T</i> = 355.0 K							
0.680	0.996315	1.5112	2.5765	4.080	0.991609	1.5627	2.9530
1.360	0.993516	1.5222	2.6533	4.760	0.993596	1.5720	3.0234
2.040	0.991622	1.5328	2.7299	5.440	0.996639	1.5809	3.0909
2.720	0.990655	1.5432	2.8057	6.120	1.000783	1.5895	3.1549
3.400	0.990640	1.5531	2.8803	6.800	1.006071	1.5977	3.2153
<i>T</i> = 370.0 K							
0.680	0.997613	1.5105	2.5722	4.080	0.999173	1.5595	2.9241
1.360	0.996096	1.5209	2.6443	4.760	1.002374	1.5684	2.9894
2.040	0.995469	1.5310	2.7161	5.440	1.006620	1.5771	3.0520
2.720	0.995754	1.5408	2.7870	6.120	1.011954	1.5854	3.1114
3.400	0.996978	1.5503	2.8564	6.800	1.018422	1.5936	3.1674
<i>T</i> = 385.0 K							
0.680	0.998793	1.5099	2.5682	4.080	1.006063	1.5567	2.8985
1.360	0.998442	1.5197	2.6363	4.760	1.010372	1.5654	2.9594
2.040	0.998968	1.5294	2.7038	5.440	1.015716	1.5738	3.0177
2.720	1.000394	1.5387	2.7702	6.120	1.022137	1.5819	3.0730
3.400	1.002748	1.5479	2.8353	6.800	1.029683	1.5900	3.1251
<i>T</i> = 400.0 K							
0.680	0.999870	1.5094	2.5647	4.080	1.012358	1.5543	2.8756
1.360	1.000585	1.5188	2.6290	4.760	1.017683	1.5627	2.9327
2.040	1.002164	1.5279	2.6927	5.440	1.024032	1.5709	2.9872
2.720	1.004633	1.5369	2.7552	6.120	1.031451	1.5789	3.0389
3.400	1.008020	1.5457	2.8163	6.800	1.039983	1.5867	3.0876
<i>T</i> = 415.0 K							
0.680	1.000857	1.5090	2.5615	4.080	1.018130	1.5522	2.8551
1.360	1.002547	1.5179	2.6225	4.760	1.024386	1.5604	2.9087
2.040	1.005091	1.5267	2.6826	5.440	1.031660	1.5683	2.9600
2.720	1.008516	1.5353	2.7417	6.120	1.039994	1.5762	3.0085
3.400	1.012852	1.5438	2.7993	6.800	1.049433	1.5838	3.0542
<i>T</i> = 430.0 K							
0.680	1.001764	1.5087	2.5586	4.080	1.023436	1.5503	2.8365
1.360	1.004350	1.5172	2.6166	4.760	1.030551	1.5583	2.8871
2.040	1.007781	1.5256	2.6736	5.440	1.038676	1.5661	2.9355
2.720	1.012086	1.5339	2.7294	6.120	1.047854	1.5737	2.9812
3.400	1.017293	1.5422	2.7838	6.800	1.058129	1.5811	3.0242

Table I. (Continued)

ρ_n (mol·dm ⁻³)	Z	$C_{v,m}/R$	$C_{p,m}/R$	ρ_n (mol·dm ⁻³)	Z	$C_{v,m}/R$	$C_{p,m}/R$
$T = 450.0$ K							
0.680	1.002863	1.5083	2.5552	4.080	1.029874	1.5480	2.8143
1.360	1.006536	1.5164	2.6095	4.760	1.038031	1.5558	2.8614
2.040	1.011044	1.5243	2.6627	5.440	1.047192	1.5635	2.9064
2.720	1.016415	1.5323	2.7147	6.120	1.057398	1.5709	2.9489
3.400	1.022681	1.5401	2.7653	6.800	1.068692	1.5779	2.9889

increases to about $\pm 0.2\%$. These estimated uncertainties cannot be applied with confidence at pressures above 20 MPa, as these correspond to the region in which u was extrapolated; nevertheless, we speculate that the likely errors do not in fact exceed the given uncertainties. Finally, in Fig. 4 we compare our values of $C_{p,m}$ with values obtained from the IUPAC equation of state [8] and with recent experimental values [9]. The agreement is generally within the claimed uncertainty of the literature values, but since this exceeds the present uncertainty by a factor of about 10, the comparison is not particularly informative.

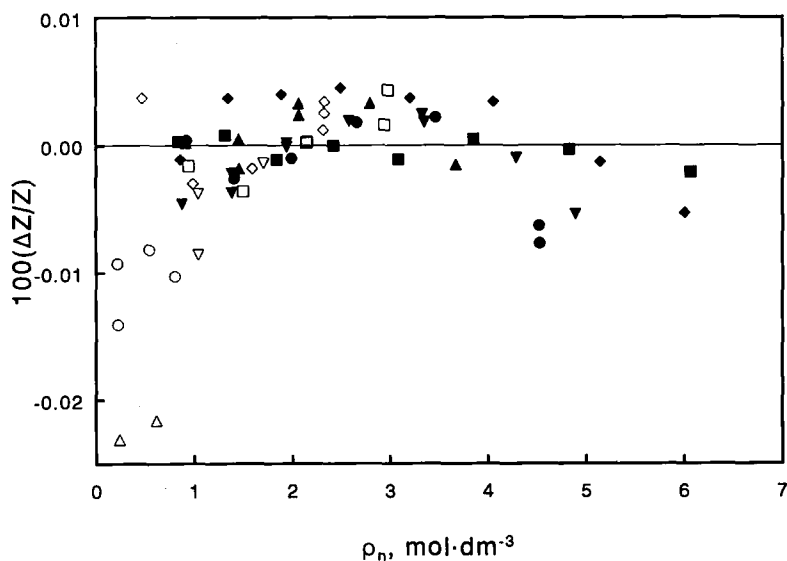


Fig. 1. Fractional deviations $\Delta Z/Z$ of the compression factors Z reported by Gilgen et al. [2] from the present results for temperatures between 110 and 153 K. ■, 153 K; ◆, 150.7 K; ▼, 148 K; ●, 146 K; ▲, 143 K; □, 140 K; ◇, 135 K; ▽, 130 K; ○, 120 K; △, 110 K.

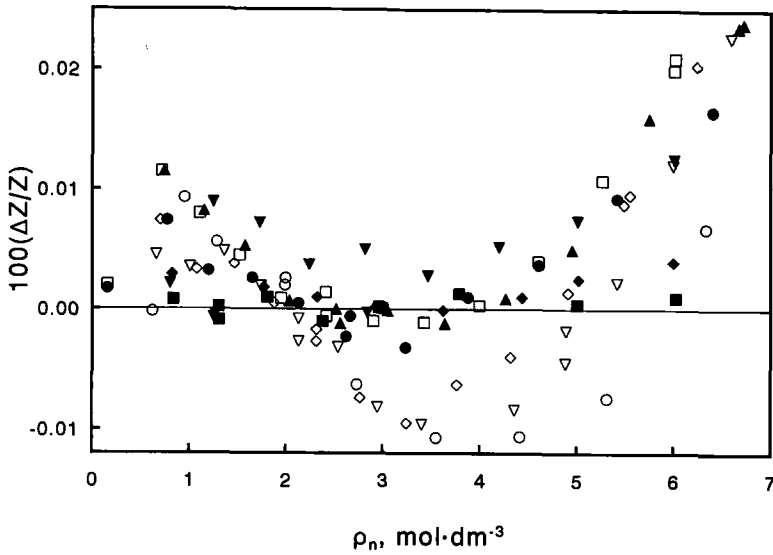


Fig. 2. Fractional deviations $\Delta Z/Z$ of the compression factors Z reported by Gilgen et al. [2] from the present results for temperatures between 154 and 200 K. ■, 155 K; ◆, 157 K; ▼, 160 K; ●, 165 K; ▲, 170 K; □, 175 K; ◇, 180 K; ▽, 190 K; ○, 200 K.

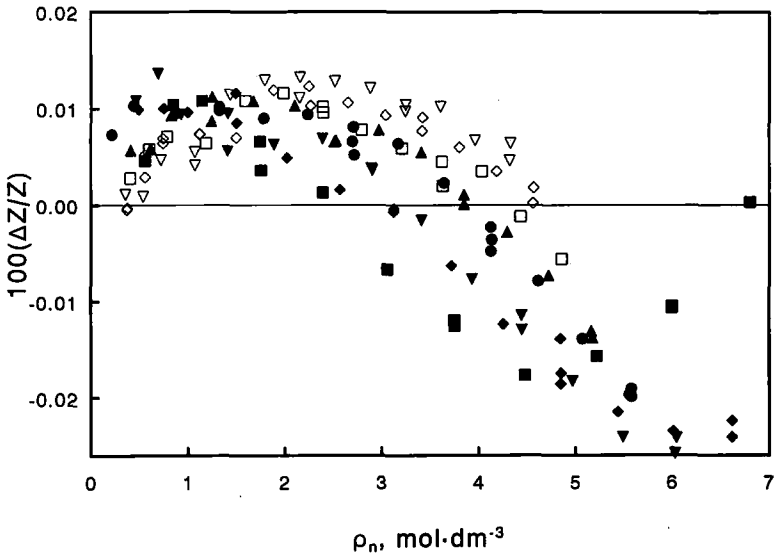


Fig. 3. Fractional deviations $\Delta Z/Z$ of the compression factors Z reported by Gilgen et al. [2] from the present results for temperatures between 220 K and 340 K. ■, 220 K; ◆, 250 K; ▼, 265 K; ●, 280 K; ▲, 295 K; □, 310 K; ◇, 325 K; ▽, 340 K.

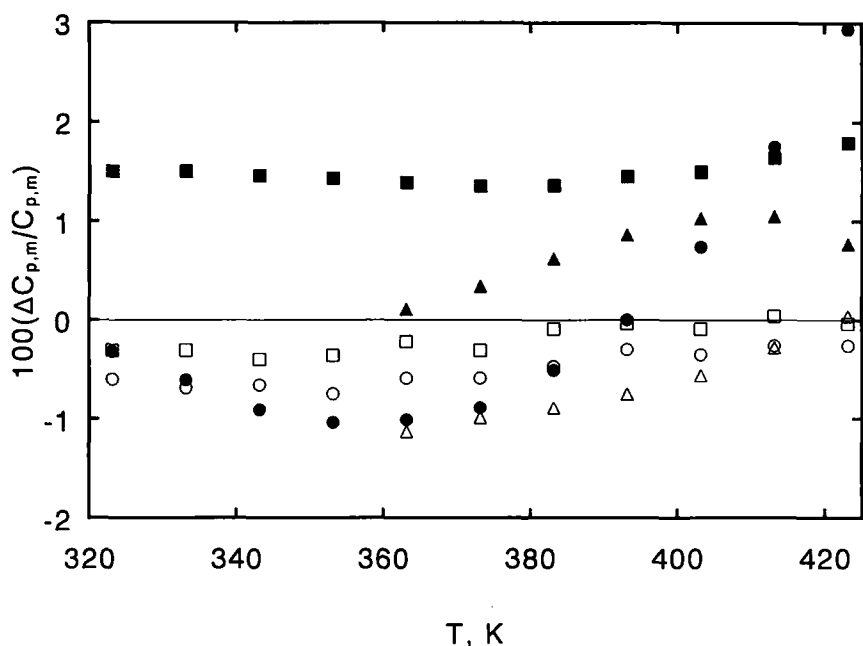


Fig. 4. Fractional deviations $\Delta C_{p,m}/C_{p,m}$ of isobaric molar heat capacities $C_{p,m}$ from the present results. Open and filled symbols are from Refs. 8 and 9, respectively. ■, 5.0 MPa; ●, 9.9 MPa; ▲, 20.7 MPa; □, 5.0 MPa; ○, 9.9 MPa; △, 20.7 MPa.

7. CONCLUSIONS

The results presented in this paper are valuable in their own right, particularly as they establish with good accuracy the isochoric and isobaric heat capacity of the gas over a wide range of conditions. In the region of overlap with the results of Gilgen et al., our derived compression factors have an estimated uncertainty only slightly greater than theirs and our results extend to both higher temperatures and higher pressures. The approach followed here is formally exact and does not assume any functional form for the thermodynamic properties (except in the region where u was extrapolated). The main limitation on the accuracy of the results is that imposed by the accuracy with which the initial conditions are known. Apart from Trusler and Zarari [5], who applied similar methods to methane, other attempts to obtain thermodynamic properties of compressed gases from the speed of sound have involved severe approximations [10, 11]. In due course we expect that a wide-ranging equation of state will be developed for the fluid state of argon. The derived properties given in

this paper are thermodynamically consistent with u and represent a linearization of the acoustic results that would permit their inclusion in a linear regression analysis to determine an empirical approximation to the Helmholtz free energy. We suggest that this approach would be of advantage.

ACKNOWLEDGMENT

A.F.E.-A. wishes to thank CONACyT for financial support during the development of this work.

REFERENCES

1. A. F. Estrada-Alexanders and J. P. M. Trusler, *J. Chem. Thermodyn.* **27**:1075 (1995).
2. R. Gilgen, R. Kleinrahm, and W. Wagner, *J. Chem. Thermodyn.* **26**:383 (1994).
3. A. F. Estrada-Alexanders, J. P. M. Trusler, and M. P. Zarari, *Int. J. Thermophys.* **16**:663 (1995).
4. J. P. M. Trusler, *Physical Acoustics and Metrology of Fluids* (Adam Hilger, Bristol, 1991), pp. 7–10.
5. J. P. M. Trusler and M. Zarari, *J. Chem. Thermodyn.* **24**:973 (1992).
6. M. L. McGlashan, *Chemical Thermodynamics* (Academic Press, London, 1979), p. 205.
7. R. B. Stewart, R. T. Jacobsen, and J. H. Becker, *Center for Applied ThermoStudies Report No. 81-3* (University of Idaho, 1981). See also B. A. Younglove, *J. Phys. Chem. Ref Data Suppl.* **11** (1982).
8. S. Angus and B. Armstrong (eds.) *International Thermodynamic Tables of the Fluid State—1. Argon* (Butterworths, London, 1971).
9. M. Baba, L. Dordain, J.-Y. Coxam, and J.-P. E. Grolier, *Indian J. Technol.* **30**:553 (1992).
10. M. R. Riazi and G. A. Mansoori, *Fluid Phase Equil.* **90**:251 (1993).
11. C. A. ten Seldam and S. N. Biswas, *J. Chem. Phys.* **94**:2130 (1991).